IMPACT OF HUMIDITY DATA ON THE PREDICTION OF ONSET VORTEX WITH A LIMITED AREA MODEL

Anuradha Kulkarni, S. S. Vaidya and *S. S. Singh*

Indian Institute of Tropical Meteorology, Pune-411008, India

Received February 11, 1992

ABSTRACT

A limited area model has been applied to study the impact of satellite-derived relative humidity data on the prediction of onset vortex of monsoon 1979. The results show that inclusion of satellite-derived relative humidity data improved the prediction of track of the cyclonic circulation and the rainfall rates in the region of the vortex.

Key words: relative humidity, onset vortex, limited area model, short-range prediction

I INTRODUCTION

Recently a few limited area primitive equation models in research mode have been formulated and applied for short-range prediction of certain aspects of summer monsoon over the Indian subcontinent (Singh, 1985; Singh et al., 1990; Krishnamurti and Ramanathan, 1982; Krishnamurti et al., 1981; Mohanty et al., 1989, 1990; Bohra, 1990). The limited area models have shown promise in simulation and prediction of large-scale monsoon features.

In this paper, a five-level primitive equation model (Singh, 1985) has been used to predict the onset vortex of 1979. Further, the impact of satellite derived moisture data on the model prediction has also been investigated.

II ONSET VORTEX OF 1979

For the present study, we selected a case of onset vortex of 12 June through 19 June 1979 which formed over the Arabian sea. The onset period was marked by an intensification of the Somali jet and the formation of a cyclonic vortex on 12 June 1979. The disturbance first became evident at 700 hPa near 10°N and had a characteristic of a mid-tropospheric cyclone (Fein and Kuettner, 1980). On 14 June 1979, the circulation at middle level intensified and induced two low centres at 850 hPa and at the mean sea level. On 15 June the vortex strengthened significantly and began to move northward. On 16 June, the vortex further intensified and was declared a cyclonic storm on 18 June and continued to move west-north-westward, weakened rapidly and landed on the coast of Oman at 12 GMT of 20 June and dissipated at 00 GMT of 21 June 1979. The onset vortex had a life history of about 10 days from 12 to 21 June 1979. The observed track of the vortex from 15 through 18 June 1979 at 850 hPa is given in Fig.1.

The FGGE level IIIb data (SOP-II) of 15 through 18 June 1979 was used as input to the model. One of the principal reasons for the choice was the high volume of data and excellent resolution.

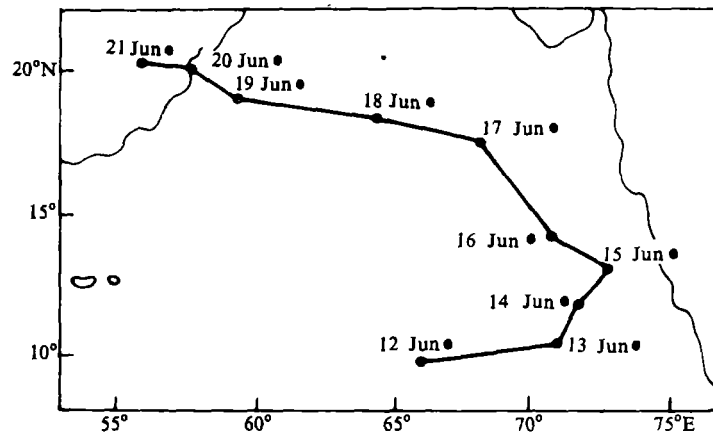

Fig. 1. Observed track of onset vortex at 850 hPa, 12 GMT, 12 to 21 June 1979.

III. MODEL

The model (Singh, 1985) was initially formulated and tested for prediction of monsoon depression. The predicted flow patterns and movement of the depression were found satisfactory upto 24 hours. However, the rainfall rates were underpredicted. The model was subsequently applied for testing the comparative performance of two schemes of convective transfer of heat and moisture (Singh, et al., 1988). The study showed that the Kuo–convection produced better forecast rainfall rates than those produced by the moist convective adjustment scheme.

The detailed description of the model is presented in Singh (1985). The following are some of the important features of this model:

(1) Independent variables x, y, p, t.

(2) Basic variables u, v, T, q, z, ω and p_s.

(3) Basic equations include the equations of motion, mass and moisture conservation, the first law of thermodynamics and the pressure tendency equation.

(4) Leap frog time integration scheme with Asselin (1972) time filter.

(5) In vertical, standard centered differencing scheme is used.

(6) Mass and energy conserving finite difference scheme for space differential following Okamura (1975) has been used.

(7) The model physics includes air–sea interaction, cumulus parameterization, large–scale condensation, dry convection adjustment, horizontal and vertical diffusion and simulated radiation.

(8) The initial balance between mass and motion fields has been obtained through a dynamic initialization scheme.

(9) A monthly mean SST is a prescribed data set.

(10) For lateral boundary conditions, the rigid walls are specified between two outermost rows of grid points in the north and south directions where normal component vanishes, but tangential flow is permitted. In the east–west direction cyclic continuity is adopted.

IV. DOMAIN, GRID AND VERTICAL STRUCTURE OF THE MODEL

The domain of integration extends from 16°S to 36°N and 33°E to 110°E. The area is resolved into a uniform grid interval of 200 km on Mercator projection. The global data having resolution of 1.875° latitude–longitude are interpolated to the regional grid points. In the horizontal, all the variables are defined at the same grid point (non–staggered grid). In the vertical the model has four layers between 100 hPa and 900 hPa with a spacing of 200 hPa, and a fifth layer of approximately 100 hPa thickness between 900 hPa and the ground surface. The horizontal wind components and the geopotential height are specified at levels 200, 400, 600, 800 and 950 hPa and the temperature, the specific humidity and the vertical velocity are set at 300, 500, 700 and 900 hPa. Vertical velocity is assumed to be zero at the model top (= 100hPa) and computed at the lower boundary through the continuity equation. The temperature field between 950 hPa and the ground surface is extrapolated at each timestep from those at 700 and 900 hPa. In the boundary layer between 950 hPa and ground surface, zero wind shear is assumed.

V. RESULTS

Two experiments were carried out with input data of four synoptic days viz. 15 June through 18 June 1979. In both the experiments the model is integrated upto 36 hours, however, the results of 24–h forecast are presented only. The FGGE IIIb relative humidity (RH) data are used in the first input data set. This is control run and hereafter referred to as EXP–I. The second set of RH data is used following Mahajan (1990). Mahajan used satellite data for the estimation of the vertical distribution of RH at levels 850, 700 and 500 hPa by using satellite–derived radiation parameters such as albedo, outgoing longwave fluxes, absorbed solar radiation and net radiation in the vicinity of the vortex. For this purpose, multiple linear regression equations were derived from MONEX–79 upsonde and dropsonde data over the Arabian Sea for the period 11—20 June 1979. The correlation coefficients of multiple linear regression of radiosonde RH and satellite–derived radiation parameters were found significant at 1% level for 850, 700 and 500 hPa. The RMSE and error variance for all the above three levels were also less for satellite–derived RH (SATRH) fields than those of FGGE RH fields. This data set was constructed for the area extending from 50°E to 80°E and 0°N to 30°N over the Arabian Sea. The satellite RH data thus–constructed replaced the grid point values of FGGE RH at 850, 700 and 500 hPa. This RH data set is used in the second experiment and will hereafter be referred to as EXP–II. The maximum RH of 80% east of onset vortex is seen in the FGGE analysis whereas nearly saturated values of RH with maximum of 95% is seen in close vicinity of the vortex in SATRH analysis. Another maximum RH is seen off the West Coast of Indian Peninsula which could be due to the presence of trough of low from the centre of the deep vortex to southern tip of the Penisula. This trough was present from 15 June to 19 June 1979. Heavy rainfall was reported for many stations along west coast during the period. It may also be pointed out that satellite–estimated isohygrometric pattern has good agreement with the cloud picture.

1. *Wind*

Fig.2 depicts 24–h forecast wind charts of EXP–I and EXP–II, and the corresponding verification wind chart at 850 hPa in respect of 17 June 1979 as input. The model produces very satisfactorily large–scale flow features such as the cross–equatorial flow and the circulations

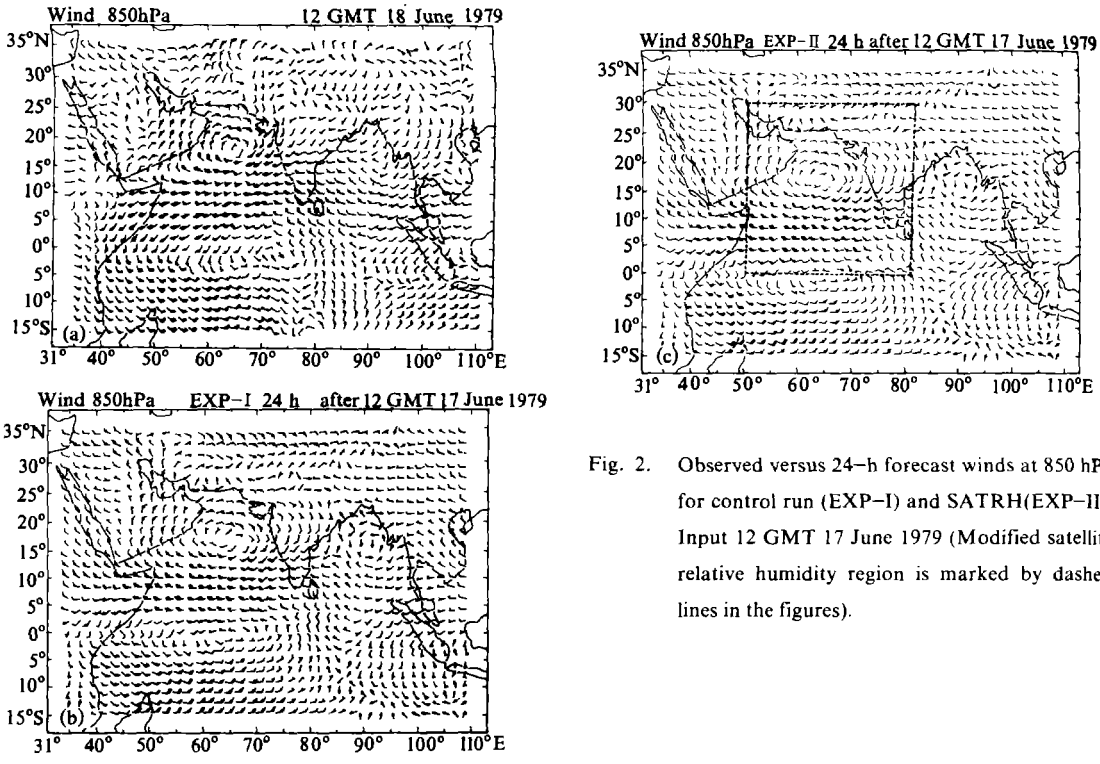

Fig. 2. Observed versus 24-h forecast winds at 850 hPa for control run (EXP-I) and SATRH(EXP-II). Input 12 GMT 17 June 1979 (Modified satellite relative humidity region is marked by dashed lines in the figures).

along the equator, whereas the low-level jet over the Arabian Sea is underpredicted. In general, the predicted easterlies to the north and westerlies to the south of the centre of the vortex are weaker in both cases. There is marginal difference in predicted large-scale flow features between EXP-I and EXP-II. Table 1 gives root mean square (RMS) errors for forecast of wind at 850 and 200 hPa levels of EXP-I and EXP-II. We find that the RMS errors are marginally smaller with the application of satellite-derived RH data.

Table 1. RMS Error for u and v (ms^{-1}) at 850 and 200 hPa Levels

Input dates	EXP-I (FGGE RH)				EXP-II (SATRH)			
	850 hPa		200 hPa		850 hPa		200 hPa	
	u	v	u	v	u	v	u	v
15 June	4.7	4.1	6.5	5.7	4.6	4.1	6.4	5.7
16 June	4.2	4.4	7.1	6.0	4.1	4.3	7.0	6.0
17 June	4.2	3.8	6.7	7.1	4.3	3.8	6.7	7.1
18 June	4.0	4.0	7.5	6.0	3.9	3.9	7.5	6.0
Mean	4.3	4.1	7.0	6.2	4.2	4.0	6.9	6.2

We further compared 24-h predicted wind by computing the differnce of u- and v- components of wind between EXP-I and EXP-II. The difference is below 0.5 m s^{-1} at most grid points except at few grid points where it is 1 m s^{-1}.

2. *Track of Onset Vortex*

Fig.3 shows the predicted and observed track of the onset vortex of 15 June through 18

June 1979. Beginning from 15 June, the vortex moved in northwest direction during 24 hours.however, the forecast movement in EXP–I was found in eastward direction. In EXP–II, the disturbance remained stationary during 24 hours. In EXP–I, with 16 June as input, no movement could be seen, whereas in EXP–II the westward movement is noticed which is somewhat realistic. With 17 and 18 June as input dates, the track is correctly predicted in both experiments. The positional vector errors from 15 June through 18 June 1979 is presented in Table 2. It may be noted from Fig.3 and Table 2 that , the satellite RH marginally improves the track forecast at initial stages of the vortex, however, in case of very intense circulation the FGGE RH is as good as SATRH as far as the movement of the onset vortex is concerned.

Impact of SATRH on the movement of vortex has been investigated by computing the vorticity advection and vorticity divergence terms of the vorticity budget equation in the vicinity of the vortex following Rajamani and Sikdar (1989). The computations were done at 850 hPa for 15 and 17 June 1979. Table 3 presents the sum of horizontal advection and vorticity divergence terms over the western and eastern halves of vortex at 850 hPa for 15 and 17 June 1979. In case of 15 June, we find negative value in the eastern half and positive value in the western half in EXP–I, resulting in generation of cyclonic vorticity in the eastern sector. The generation of cyclonic vortiçity in the eastern sector of the vortex contributed to the eastward movement of the vortex. In EXP–II, comparatively smaller positive vlaue in the western half and smaller negative value in the eastern half are found which would lead to generation of smaller magnitude of cyclonic vorticity in the eastern sector. The smaller magnitude of generation of cyclonic vorticity could have contributed to little or no eastward movement which actually has been found in EXP–II. As far as case of 17 June 1979 is concerned, we find large negative values in the western half and comparatively smaller negative values in the eastern half in both the experiments, suggesting westward movement.

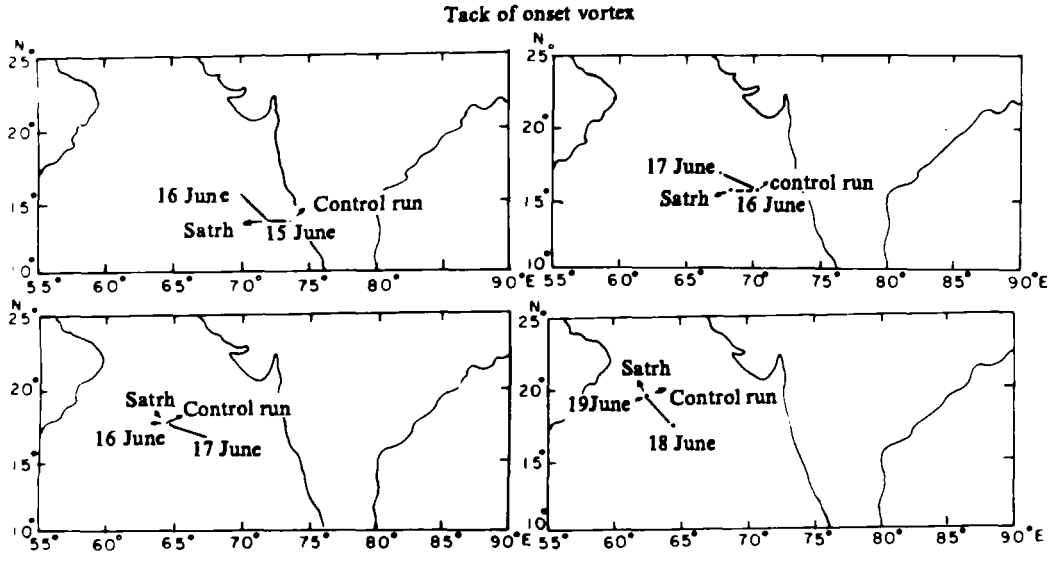

Fig. 3. Observed versus predicted tracks of the onset vortex at 850 hPa level, for control run (EXP–I) and SATRH (EXP–II). Input: 12 GMT, 15 to 18 June, 1979.

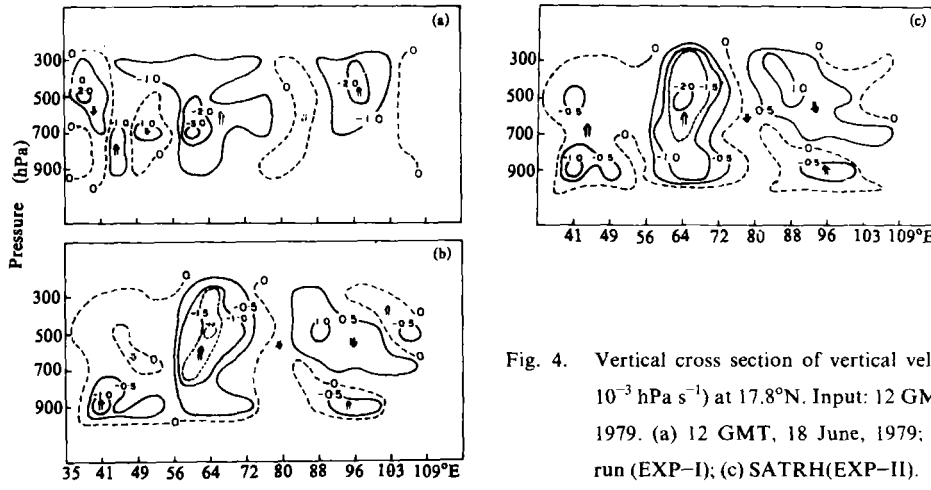

Fig. 4. Vertical cross section of vertical velocity (unit: 10^{-3} hPa s^{-1}) at 17.8°N. Input: 12 GMT, 17 June 1979. (a) 12 GMT, 18 June, 1979; (b) control run (EXP–I); (c) SATRH(EXP–II).

Table 2. Positional Error (km) for Onset Vortex

Input dates	Positional error (km) in 24 hr	
	(FGGE RH) EXP–I	(SATRH) EXP–II
15 June	370	300
16 June	300	120
17 June	0	0
18 June	0	0

Table 3. Sum of Horizontal Advection and Vorticity–divergence Terms ($10^{-12}s^{-2}$) over the Western (W) and Eastern (E) Halves of Vortex at 850 hPa Level

Input date	EXP–I		EXP–II	
	W	E	W	E
15 June	39	−39	2	−5
17 June	−89	−22	−101	−7

In the foregoing discussion, it was shown that the vorticity structure of the vortex got modified by the use of SATRH. The modified vorticity distribution in the vicinity of the vortex could be the prime cause for improvement in the forecast movement.

3. *Vertical Velocity and Rainfall*

Fig.4 shows the vertical cross–section of vertical velocity from EXP–I, EXP–II and the corresponding observed vertical velocity. It is seen that a maximum upward motion of 3×10^{-3} hPa s^{-1} occurs at 700 hPa level in the verification chart, whereas the predicted maximum vertical velocity is of the order of 2×10^{-3} hPa s^{-1} in SATRH experiment and 1.7×10^{-3} hPa s^{-1} in control run, located at 500 hPa. In general upward motion cells associated with the disturbance are predicted well in both experiments. The vertical velocity field outside the disturbance region being weak, displayed both signs and did not show good agreement with observed vertical velocity.

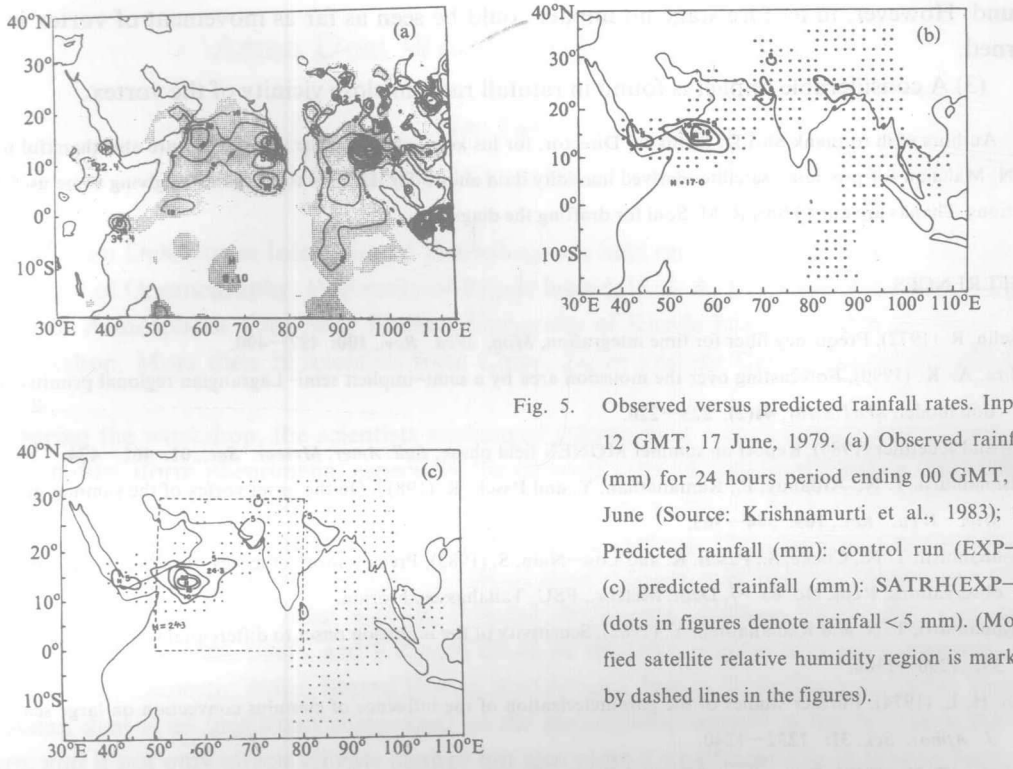

Fig. 5. Observed versus predicted rainfall rates. Input: 12 GMT, 17 June, 1979. (a) Observed rainfall (mm) for 24 hours period ending 00 GMT, 19 June (Source: Krishnamurti et al., 1983); (b) Predicted rainfall (mm): control run (EXP–I); (c) predicted rainfall (mm): SATRH(EXP–II) (dots in figures denote rainfall < 5 mm). (Modified satellite relative humidity region is marked by dashed lines in the figures).

Fig.5 presents the predicted and the corresponding observed rainfall rates for 17 June 1979 as input. Table 4 presents the observed and predicted maximum rainfall for 15—18 June 1979. It is well known that heavy rainfall occurs in southwest sector of the monsoon disturbance centre. It may be noted that the rainfall rates associated with the vortex is predicted well. In EXP–II the maximum rainfall associated with the vortex is comparable with the observed rates. As seen from Table 4, the predicted maximum rainfall rates for 15 June—18 June 1979 with EXP–II are closer to the observed rainfall rates.

Table 4. Maximum Rainfall (mm / 24 h) Associated with the Onset Vortex

Input dates	Maximum Rainfall (mm / 24 h)		
	(FGGE RH) EXP–I	(SATRH) EXP–II	Observed
15 June	2.4	8.6	35
16 June	9.4	19.3	30
17 June	17.1	24.3	35
18 June	10.2	27.3	25

VI. CONCLUSIONS

A limited area model has produced a reasonably good forecast of 1979 onset vortex as far as large–scale circulation features are concerned. The impact of satellite–derived humidity data on prediction of onset vortex are the following:

(1) There is marginal impact on large–scale flow features.

(2) A positive impact on the prediction of movement of onset vortex during early stage was found. However, in mature stage no impact could be seen as far as movement of vortex is concerned.

(3) A considerable impact is found in rainfall rates in close vicinity of the vortex.

Authors wish to thank Shri D. R. Sikka, Director, for his keen interest in the study. They are also thankful to Shri P. N. Mahajan for providing satellite-derived humidity data and to Dr. D. Subrahmanyam for giving some useful suggestions. Thanks are due to Shri R. M. Soni for drafting the diagrams.

REFERENCES

Asselin, R. (1972), Frequency filter for time integration, *Mon. Wea. Rev.*, **100:** 487—490.

Bohra, A. K. (1990), Forecasting over the monsoon area by a semi-implicit semi-Lagrangian regional primitive equation model, *MAUSAM*, **41(2)**: 223—226.

Fein and Kuettner (1980), Report on summer MONEX field phase, *Bull. Amer. Meteor. Soc.*, **61**: 461—474.

Krishnamurti, T. N., Ardanuy, P., Ramanathan, Y. and Pasch, R. (1981), On the onset vortex of the summer monsoon, *Mon. Wea. Rev.*, **109:** 344—363.

Krishnamurti, T. N., Cocke, S., Pasch, R. and Low-Nam, S. (1983), Precipitation estimates from raingauge and satellite observations; Rept. No. 83—7, Dept. Meteor., FSU, Tallahassee, Florida.

Krishnamurti, T. N. and Ramanathan, Y. (1982), Sensitivity of the monsoon onset to differential heating, *J. Atmos. Sci.*, **39:** 1290—1306.

Kuo, H. L. (1974), Further studies of the parameterization of the influence of cumulus convection on large scale flow, *J. Atmos. Sci.*, **31:** 1232—1240.

Mahajan, P. N. (1990), Estimation of vertical distribution of relative humidity using satellite data, *Acta Meteorologica Sinica*, **4:** 231—238.

Mohanty, U. C., Paliwal, R. K., Tyagi, A. and John, A. (1989), Evaluation of a multi-level primitive equation limited area model for short range prediction over Indian region, *MAUSAM*, **40:** 29—36.

Mohanty, U. C., Paliwal, R. K., Tyagi, A. and John, A. (1990), Evaluation of a limited area model for short range prediction over Indian region, Sensitivity studies. *MAUSAM*, **41(2)**: 251—256.

Okamura, Y. (1975), Computational design of a limited area prediction model, *J. Meteor. Soc.*, Japan, **53**: 175—188.

Rajamani, S. and Sikdar, D. N. (1989), Some dynamical characteristics and thermal structure of monsoon depressions over the Bay of Bengal, *Tellus*, **41A**: 255—269.

Singh, S. S. (1985), Short range prediction with a multi-level primitive equation model, *Proc. Indian Acad. Sci.*(Earth and Planet Sci.), **94**: 159—184.

Singh, S. S., Bandyopadhyay, A. and Vaidya, S. S. (1988), Impact of convective transfer of heat and moisture on the prediction of monsoon depressions, *MAUSAM*, **39(1)**: 19—26.

Singh, S. S., Vaidya, S. S. and Rajagopal, E. N. (1990), A limited area model for monsoon prediction, *Advances in Atmos. Sci.*, **7(1)**: 111—126.